Observations of Hurricane Sandy from a Glider Mounted Aquadopp Profiler

Travis Miles, Scott Glenn, Josh Kohut, Greg Seroka, Yi Xu
Rutgers University
Institute of Marine and Coastal Sciences
New Brunswick, NJ, 08901, USA
tnmiles@marine.rutgers.edu

***Abstract*—The Middle Atlantic Bight (MAB) has been experienced numerous extra-tropical cyclones and hurricanes in recent years that have cauased extensive damage along the New York and New Jersey coastlines. Understanding the coastal ocean ahead of such events is critical to accurately forecasting storm intensity. On the MAB in summer temperatures can vary by over 14 ^{o}C from the surface to bottom due to the presence of the summer Cold Pool. These cold bottom waters have the potential to weaken storms as they cross the shallow continental shelf. Despite the importance of understanding the dynamics ahead of and beneath these storms observations, the extreme conditions limit our ability to observe the coastal ocean response and potential atmospheric feedbacks. In order to resolve the coastal ocean response we deployed two Teledyne-Webb Slocum gliders ahead of Hurricane Sandy in October 2012, the second costliest hurricane in United States history. One glider, RU23, was equipped with a Nortek Aquadopp current profiler with a custom glider transducer head. Ahead of Hurricane Sandy we two-layer cross-shelf flow consisted with a downwelling circulation. As the downwelling front was advected offshore past the glider location two-layer cross-shelf flow shifted to one-layer along-shelf flow. With the offshore advection of cold bottom water there was no available cold water to mix to the surface and reduce the impact of Hurricane Sandy as it crossed the shelf.**

Keywords— *Ocean Observing, Autonomous Underwater Vehicles, gliders, current profilers, hurricanes.*

I. INTRODUCTION

In recent years hurricanes and extra-tropical cyclones have frequently impacted the Middle Atlantic Bight (MAB) and caused extensive damage to cities and coastal communities. These storms are important episodic events for sediment transport [1,2,3,4,5], coastal ocean mixing and could play a critical role in initiating the fall phytoplankton bloom directly [6] or indirectly by eroding the summer stratification and allowing nutrients to replenish the shallow coastal ocean [7]. Despite the importance of such events, the available observations of the coastal ocean response to theses storms are rare, primarily due to difficulty in safely sampling such violent conditions. While observations are limited, the importance of these measurements for accurate storm forecasts is critical.

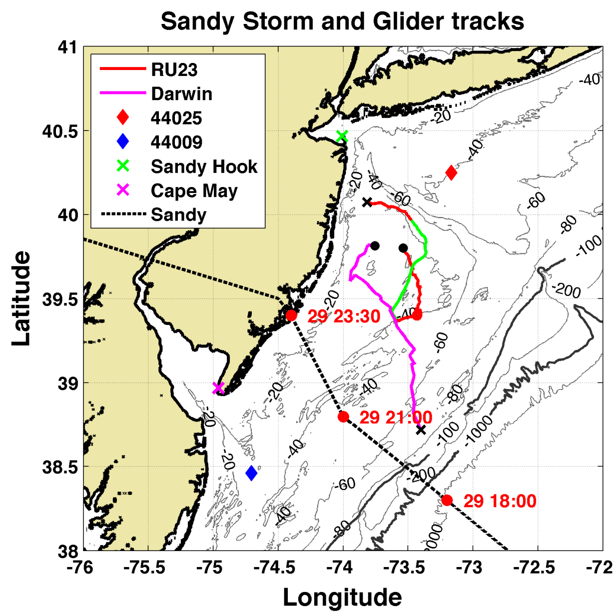

Fig 1. Map of the Middle Atlantic Bight study region with the RU23 glider track (red), RU23 glider track during the storm forcing period from October 28th at 00:00 GMT to October 31st at 00:00 GMT (green), Darwin glider track (magenta), buoys 44025 (red diamond) and 44009 (blue diamond), tide gauge stations at Sandy Hook (green x) and Cape May (magenta x) and NHC best track for Hurricane Sandy (black dashed) with times listed in red.

Emanuel et al. [8] and others [9,10] have detailed the importance of sea-surface temperature measurements beneath storms as drops of 1-2^{o}C can lead to significant storm weakening and a recent paper [11] suggests that understanding the full water-column temperature structure ahead of a storm is critical to improving storm intensity forecasts. Despite these recent advances few of these papers detail the continental shelf response just prior to landfall.

Observations in large storms are commonly made by airborne expendable bathythermograph (AXBT) [12] deployed from aircraft further offshore, while these data are invaluable for determining storm development they provide limited information about the time evolution of the coastal ocean during storms, particularly on continental shelves just prior to landfall.

978-0-933957-40-4 ©2013 MTS

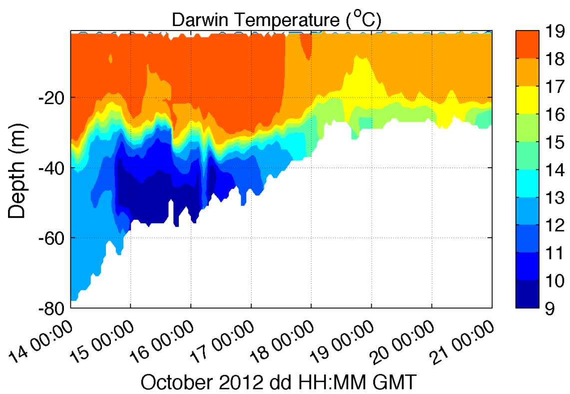

Fig 2. Glider RU23's Temperature cross-shelf section from the shelf break to the near-shore a week before Hurricane Sandy made landfall.

Previous studies have used opportunistically placed moorings such as the array in [13] on the continental slope or data from cabled observatories in [14]. While data from these systems are critical to understanding storm development, they rely on placement weeks to months before storms, cannot be adapted based on storm track forecasts and can be expensive to maintain. Recent studies have used autonomous-underwater-vehicles, specifically Teledyne-Webb Slocum gliders to adaptively sample the coastal water-column before, during and after storms in a variety of regions and conditions [1, 2, 15]. These instruments have not only provided a wealth of data, but they are capable of real-time data transmission that may be assimilated into ocean models and assist in emergency management decision making [16].

Hurricane Sandy developed as a tropical wave off the coast of Africa on October 11th, made landfall in Jamaica as a category 1 hurricane on October 24th and a category 3 hurricane in Cuba on October 25th. Sandy then ran parallel to the east coast of the United States until it made a turn toward the west-northwest and made landfall just north of Atlantic City, NJ at 23:30 GMT on October 29th. Historic storm surges along the NJ and NY coastlines have lead to Sandy being named the second costliest storm in U.S. history, with an estimated $68 Billion in damages (National Weather Service http://www.nws.noaa.gov/os/assessments/). On October 25th, 2012, while Sandy was still in the Caribbean we deployed a Teledyne-Webb coastal ocean glider equipped with a suite of hydrographic sensors, including an experimental Nortek Aquadopp Current Profiler. In this paper we detail not only the temperature evolution of the water-column beneath Sandy, but also the time-evolution of the current structure beneath the storm.

II. Methods

A. Instrumentation

Teledyne-Webb Research Slocum Gliders (gliders) are buoyancy driven autonomous underwater vehicles that are essentially mobile profiling sensor platforms, with interchangeable science bays [16]. Gliders have a proven history of sampling in extreme weather conditions, [1, 2, 15] Two gliders provided data for this study. Darwin performed a cross-shelf transect of the continental shelf from the shelf-break to just off Tuckerton, NJ, (Fig 1) between October 14th and 21st and was equipped with a standard Seabird Electronics (SBE) conductivity, temperature and depth (CTD) sensor and Wetlabs Ecopuck, which uses fluorescence to estimate Chlorophyll concentration. RU23 was deployed 15 km of offshore southeast of Sandy Hook, NJ, (Fig 1) on October 25th, as forecasts indicated Hurricane Sandy would approach the MAB. RU23 was also equipped with an SBE-CTD and Wetlabs Ecopuck as well as an additional Optical Backscatter puck (BB3). The BB3 measures optical backscatter at three wavelengths, 470, 532 and 660 nanometers, and serves as a proxy for suspended sediment concentration.

To measure water-column currents a Nortek Aquadopp Current Profiler (Aquadopp) with a custom glider head was mounted on RU23 in an upward looking position and logged data internally. The Aquadopp was tuned to collect data in beam coordinates in 1 meter bins with a beam length of 10 meters. On downcasts with a glider pitch angle of ~ 26.5^{o} degrees the Aquadopp had a pitch angle of 0^{o}. We employ a shear-least squares method originally detailed in [17] for profiling current profilers and adapted for use on autonomous platforms in [18] in order to calculate realistic currents from the glider mounted Aquadopp.

We calculate water-column shear at one meter intervals on downcasts only, and use a combination of pitch angle, heading and expected and actual dive and surface locations, known as dead-reckoning [19] to reference the mean water-column velocity. We programmed RU23 to surface at hourly intervals in order to increase depth-averaged data resolution. All glider and Aquadopp data were interpolated to one hour and one meter bins using a Gaussian weighting function with 1 m vertical radius and 1 hour temporal radius. We used least squares to remove the barotropic tidal component from all depth bins. Glider currents as well as winds at buoy locations are rotated 30 degrees clockwise from North to align approximately along-shore on New Jersey Shelf.

Atmospheric data from a combination of buoys and models, coastal water-level data from coastal tide gauges and surface currents from CODAR High-Frequency Radar supplemented glider measurements. Buoy data were obtained from National Oceanographic and Atmospheric Association (NOAA) National Data Buoy Center (NDBC) buoys 44009 off Delaware Bay, 44025 off Long Island and 44065 in Hudson Bay. These buoys included standard meteorological data including atmospheric pressure, temperature, winds, wave-heights, wave-period wave-direction and sea-surface temperature (SST).

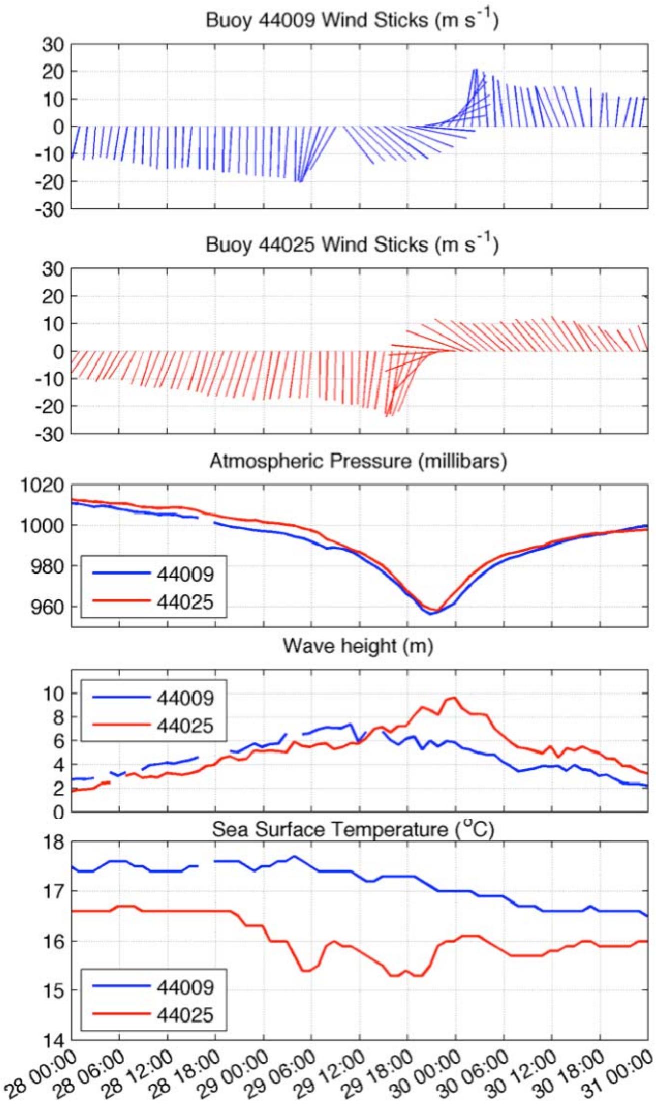

Fig 3. Data from NOAA buoys 44009 (blue) and 44025(red) with wind speed and directions (toward) in the upper two panels, atmospheric pressure in the third panel, wave heights in the fourth panel and sea surface temperature in the bottom panel.

We extract wind stress data in the vicinity of the glider from the North American Mesoscale (NAM) forecast system and validate these data against wind stress at buoy 44025 calculated from [20] to account for reductions in wind stress at high wind speed. Water-level data was obtained from two locations, Sandy Hook, NJ, Atlantic City, NJ and Battery Park, NY. CODAR Ocean Sensors SeaSonde HF Radar system measures surface currents on the MAB. Descriptions of the CODAR data and its shelf-wide applications are outlined in [21] and [22]. The network provides surface current observations at the estimated equivalent depth of 2.4 m [23].

B. Depth Averaged Momentum Balance

Previous studies [14, 24, 25 26] have used the depth-averaged momentum equations to detail the near-shore coastal ocean response to atmospheric forcing. The study [14] uses these equations off the New Jersey Shelf during Tropical Storm Floyd. Similar to this study we assume the nonlinear terms are small and use the following governing equations

(1) $$\frac{\partial u}{\partial t} = -g\frac{\partial \eta}{\partial x} + fv + \frac{\tau_{wx}}{\rho H} - \frac{\tau_{bx}}{\rho H}$$

(2) $$\frac{\partial v}{\partial t} = -g\frac{\partial \eta}{\partial y} - fu + \frac{\tau_{wy}}{\rho H} - \frac{\tau_{by}}{\rho H}$$

With u and v as the cross-shore and along-shore depth-averaged velocities, g is gravity, *n* is the sea-surface height assuming a barotropic pressure gradient, *f* is the coriolis frequency, H is water-depth, T_{wx} (T_{wy}) is the cross-shelf (along-shelf) wind stress and T_{bx} (T_{by}) is the cross-shelf (along-shelf) bottom stress.

We calculate wind stress at buoy 44025 following [20] for high-wind conditions and use it to validate wind stress extracted from the NAM model in the vicinity of the glider location. The magnitude of the NAM and 44025 wind stresses were correlated with a 0.96 correlation coefficient during the forcing period. To calculate depth averaged wind stress we divide the surface wind stress from NAM along the glider track by the glider observed water-column depth.

Our Aquadopp was oriented in an upward-looking position so as not to obstruct measurements by the Ecopuck or BB3. The upward looking orientation results in the lowest depth-bin measured approximately a meter above the glider and limits our proximity and data near the bottom as the glider must begin to inflect within ~3m of the bottom. This makes observed log-profiles during extreme forcing conditions difficult to obtain from a moving platform. Bottom stress can be represented as

(3) $$\tau_b = \rho u_*^2$$

where u_* is the friction velocity. With a linear eddy viscosity and a constant stress layer

(4) $$u_* = u(z)\kappa / \ln\frac{z}{z_0}$$

Where *u(z)* is a near-bottom velocity at depth *z*, *k* is Von Karman's constant of 0.4 and z_0 is the roughness length scale. Determination of z_0 has been the subject of numerous studies over the past 40 years. As we are only attempting to estimate the force balances we used a roughness length z_0 of 0.1 cm similar to a study by [27] on the southern MAB and determine u_* from velocities and directions measured 5 meters off the bottom. Future studies should include downward looking current profilers in order to obtain more data in much closer proximity to the bottom. Validation in the vicinity of the bottom with more traditional bottom mounted current profilers or tripod systems are necessary.

Local tide gauges showed historic coastal storm surges along the MAB indicating that sea-surface slope could not be neglected. We could not measure the slope directly in the vicinity of the glider, but we estimate the magnitude of the sea-surface slope from the coastal tide gauges and compare them to the inferred slope calculated by the residual necessary to balance the depth-averaged momentum equations. All forces were filtered with a 20-hour lowpass filter to highlight the large scale storm forcing.

Coriolis and acceleration forces were calculated directly from the depth-averaged glider velocities. We use a Coriolis frequency, *f*, of 10^{-4} to estimate the Coriolis force. Along- and cross-shelf acceleration was calculated by taking the hourly centered difference of the cross- and along- shelf depth-averaged velocities.

III. Observations

Five days prior to the storm Darwin sampled surface temperatures over 18°C with a deep upper-mixed layer (~30 m) and sampled the remnant summer Cold Pool water (citation) that extended from the 60m isobath to just in-shore of the 40 m isobath, with temperatures ranging from 9-13C. The inner-shelf, shoreward of the 30 m isobath was warm (> 18°C) and well-mixed (Fig 2). Glider RU23 was deployed on October 25th, 15 km offshore of northern, NJ (Fig 1) and transited southward along the 40 meter isobath. The eye of Hurricane Sandy was mapped from The National Hurricane Center best track (Fig 1).

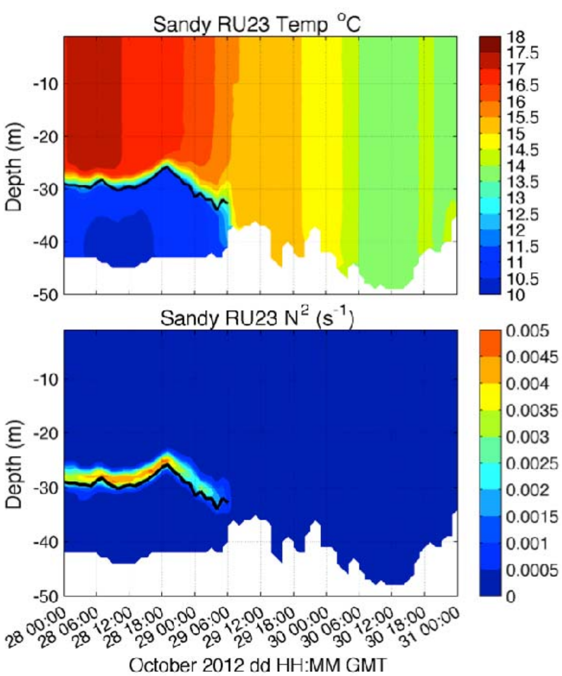

Fig 4. Glider RU23 cross-sections of temperature (upper panel) and buoyancy frequency (lower panel) while transiting approximately along the 40 meter isobath. The solid black line in both figures is the measured mixed-layer depth.

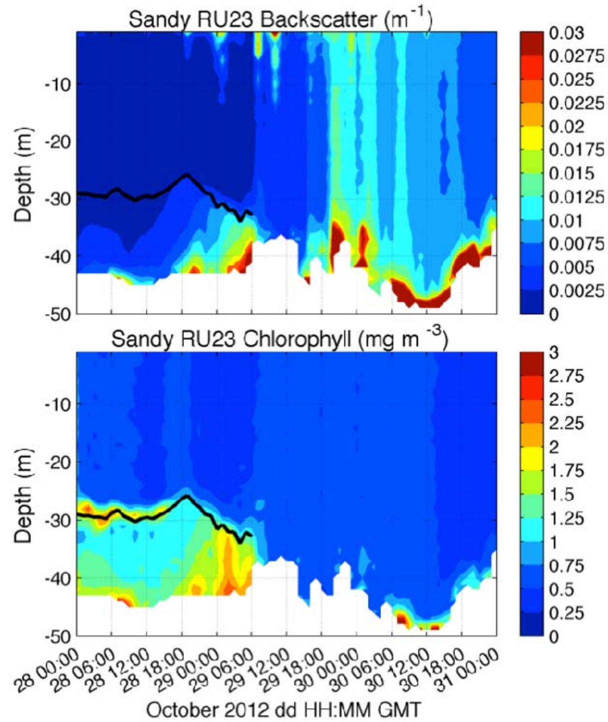

Fig 5. Glider RU23 cross-sections of optical backscatter at 470 nm wavelength (upper panel) and chlorophyll concentration (lower panel) while transiting approximately along the 40 meter isobath. The solid black line in both figures is the measured mixed-layer depth.

The eye passed between buoys 44009 and 44025, less than 50 kilometers south of RU23. Winds began to increase in intensity at buoy 44009 and 44025 (Fig 3) late on October 27th while the storm was off the continental shelf parallel to Florida. Winds were initially uniformly oriented along-shelf and downwelling favorable at both locations. As the storm passed between both buoys the winds rotated opposite directions, counter-clockwise and clockwise at 44009 and 44025 respectively, with the strongest winds on the north side of the storm, consistent with previous studies. Cross-sections of RU23 temperature (Fig 4) show that surface temperatures at the glider location dropped from 17°C at 00:00 GMT on the 28th to a minimum of 14°C at 12:00 GMT on the 30th. Glider bottom temperatures warmed rapidly on the 29th between 00:00 and 8:00 GMT. At the buoy locations, SST response to the storm was weaker with cooling of only 1-2C over the same period (Fig 3). Cross-sections of RU23 temperature (Fig 4) show the thermocline initially shoaled between 12:00 and 19:00 GMT on the 28th, and then deepened between 19:00 GMT on the 28th and 06:00 GMT on the 29th when the full water-column became well-mixed. Buoyancy frequencies were calculated from temperature and a mean representative salinity of 32.5, as thermal-lag significantly impacted salinity measurements across the thermocline and temperature was the dominant source of stratification. Buoyancy frequencies were at a maximum just above the thermocline (Fig 4) and remained elevated until the water-column was well mixed on the 28th at 06:00 GMT.

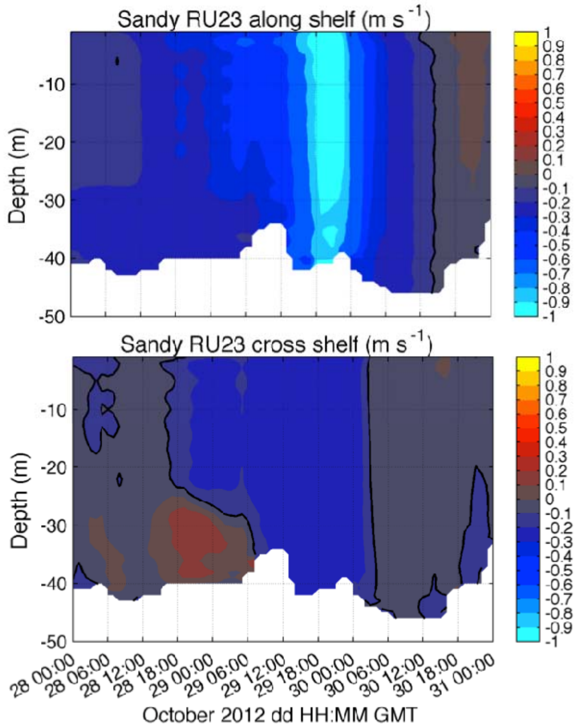

Fig 6. Glider RU23 Aquadopp Current Profiler cross-sections of detided along-shelf velocity (upper panel) and detided cross-shelf velocity (lower panel) while transiting approximately along the 40 meter isobath. The solid black line in both figures is the 0 line, with warmer colors being positive northeastward (offshore) in the along-shelf (cross-shelf). Currents were rotated 30 degress clockwise from north to be approximately along- and cross- shelf.

Optical backscatter at 470 nm^{-1} was enhanced below the thermocline (Fig 5) at 06:00 GMT on the 28th, and was restricted below the thermocline until after the water-column was well-mixed and sediment was re-suspended uniformly to the surface at 19:00 GMT on the 29th. Sediment resuspension has been observed from gliders in the past (Glenn et al., 2008; Miles et al., 2012). Sediment resuspension is driven by wave-induced bottom orbital velocities, which, following linear wave theory are high at large wave-heights on the continental shelf [28]. Wave heights during Hurricane Sandy are over 5 m at both buoys 44009 and 44025 (Fig 3) during the initial resuspension prior to stratification breaking down. The restriction of sediment below the thermocline indicates that while wave-induced bottom stresses are likely high, water-column turbulence is not strong enough to mix sediment across the thermocline.

Chlorophyll concentrations were elevated below the thermocline (Fig 5). Though light is available, nutrients in late summer to early fall are depleted in the warm surface waters and can only be accessed in areas where the nutrient rich Cold Pool remains in the euphotic zone (citation). Similar to sediment chlorophyll is not mixed across the stable thermocline.

Observed along-shore glider currents between October 28th at 00:00 GMT and the 29th at 06:00 GMT (Fig 6) were primarily aligned toward the southwest throughout the water-column at ~ 0.4 m s^{-1}. Observed cross-shelf currents were onshore in the surface and offshore near the bottom consistent with two-layer downwelling cross-shelf circulation. After the thermocline deepened and the water-column became well-mixed, cross-shore currents transitioned from two-layer to one-layer flow onshore at ~0.25 m s^{-1}, while along-shore currents were increased toward the southwest in excess of ~1 m s^{-1}.

IV. Forcing

The restricted sediment and stable bottom temperatures until October 29th after 06:00 GMT indicate that stratification likely inhibited vertical mixing and that deepening of the mixed-layer was more likely due to horizontal advection than vertical mixing. We calculate Bulk Richardson numbers from

$$R_b = \frac{N^2}{(\frac{\partial u}{\partial z})^2}$$

where N^2 is the hourly maximum water-column buoyancy frequency, and $(du/dz)^2$ is the shear across the thermocline calculated from the Aquadopp. Studies have shown that mixing is likely when $R_b < 1$ or 0.25. We observe Bulk Richardson numbers (Fig 7) equal to or greater than 1 until they fall below 1 on the 28th at 18:00 GMT and below 0.25 on the 29th at 06:00 consistent with the timing of the deepening and disappearance of the thermocline, respectively. Depth integrated Chlorophyll (Fig 7) was constant near 40 mg m^{-3} until the water-column became well-mixed on the 29th at 06:00 GMT and depth integrated Chlorophyll abruptly dropped to 20 mg m^{-3}. On short time-scales (hours) Chlorophyll concentration should be conserved as growth and grazing rates generally occur over a number of days. The drop in integrated Chlorophyll concentration, restricted sediment, stable thermocline, and Richardson numbers indicate that while mixing processes may have been occurring above the thermocline, forces were not sufficient to mix across the thermocline and advection was likely responsible for the deepening and erosion of the thermocline.

The transition from a two-layer circulation with offshore flow at the bottom and onshore flow at the top to one-layer along-shore intensified, when vertical mixing process across the thermocline are not dominant, is consistent with the offshore advection of a downwelling front detailed in previous work by [25] and [29]. In their work they showed that as downwelling favorable winds advected a downwelling front offshore there was an adjusted well-mixed inner-shelf region with primarily one-layer along-shelf flow and a stratified outer-shelf region with two-layer cross-shelf circulation seaward of a downwelling front. Our glider likely sampled both the shoreward and seaward sides of the downwelling front as the front was advected offshore. The following sections detail the force balance during the transition from stratified to un-stratified conditions.

A. Cross-shelf Depth Averaged Momentum Balance

In the cross-shelf direction (Fig 8) the depth-averaged Coriolis term was large, while acceleration, wind stress and bottom stress terms were an order of magnitude smaller. The calculated cross-shelf pressure gradient was large, which indicates that there was an approximate geostrophic balance cross-shelf which drove the observed along-shelf southwestward flow. Historic sea-levels at coastal tide stations (Fig 9) support the observed pressure gradient force. CODAR surface currents prior to loss of the mid-shelf stations indicate that flow was predominantly along-shelf toward the southwest across the majority of the NJ shelf (Fig 10).

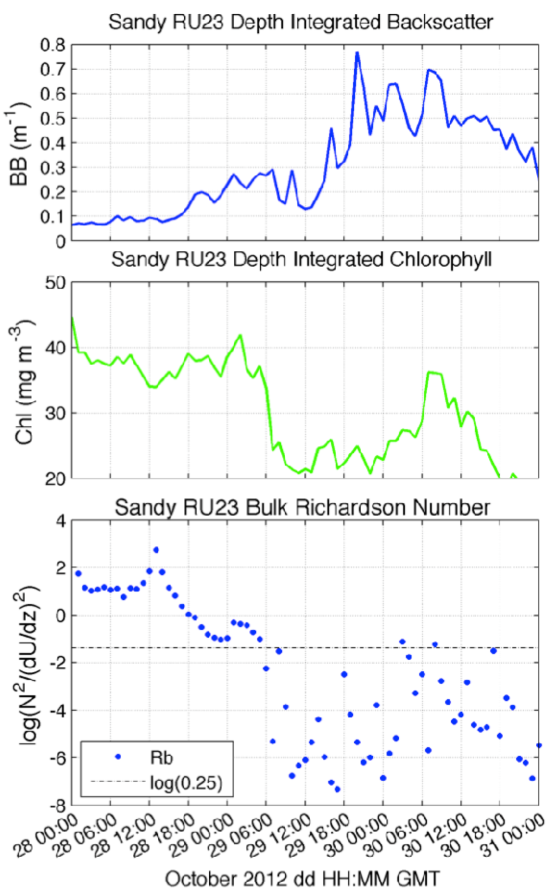

Fig 7. Glider RU23 depth integrated optical backscatter as a proxy for sediment concentration (upper panel), depth integrated chlorophyll concentration, and natural log of the bulk Richardson number. 0 on the y-axis corresponds to a bulk Richardson number of 1 and the dashed line corresponds to 0.25.

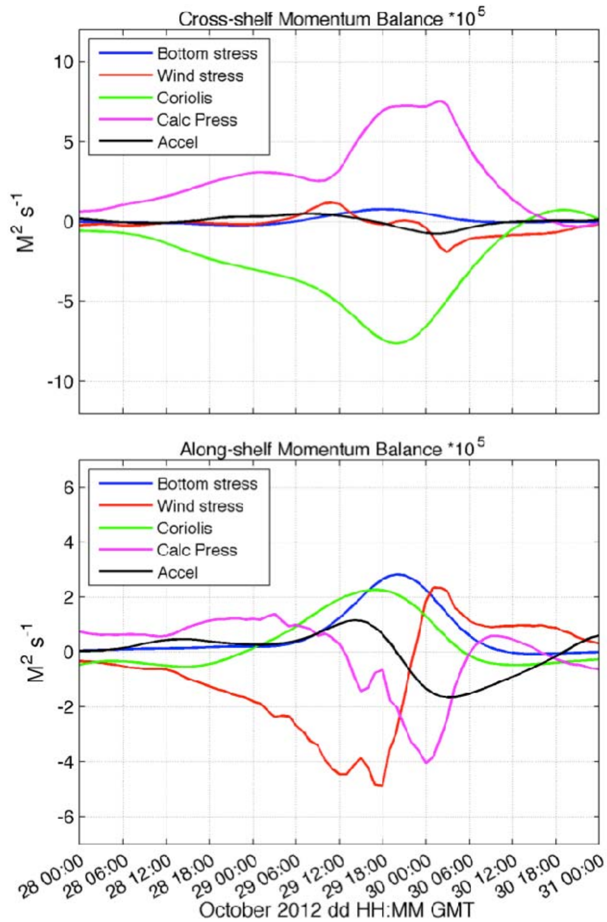

Fig 8. Estimates of the depth averaged cross-shelf (upper panel) and along-shelf (lower panel) momentum equations.

B. Along-shelf Depth Averaged Momentum Balance

As the storm approached there were clear shifts in the dominant forces in the along-shelf depth-averaged momentum balance (Fig 8). Initially a positive along-shelf pressure gradient force balanced the wind stress and Coriolis force. The strong stratification as the storm approached likely kept observed bottom stresses low. After the water-column near the glider became well-mixed, along-shelf bottom stresses quickly increased. The positive bottom-stress, Coriolis and acceleration terms balanced the negative along-shelf wind stress and pressure gradient. As the eye of the storm passed the glider location at ~18:00 GMT on the 29th acceleration terms became negative and wind stress became positive. Bottom stress remained high as the negative along-shelf pressure gradient and geostrophic cross-shelf balance continued to drive currents along-shelf toward the southwest.

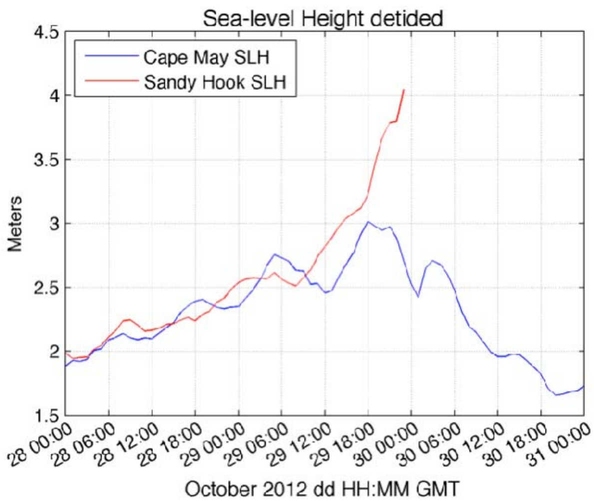

Fig 9. Sea-level height at Cape May (blue) and Sandy Hook (red), NJ, from NOAA tide gauges, with tides removed.

Again, in order to validate the calculated along-shelf depth-averaged pressure gradient terms we compare it with a series of coastal tide gauges (Fig 9). We estimate the near-shore pressure gradient force by calculating the de-tided sea-surface slope between Sandy Hook, NJ and Cape May, NJ. At the peak of the storm-surge there was ~1 meter difference between the two locations, which were separated by ~200 kilometers. This results in an estimated peak PRESSURE GRADIENT FORCE of $6x10^5$ m^2 s^{-1}, on the same order of magnitude and similarly timed as the calculated PRESSURE GRADIENT FORCE at the glider location. Additionally, Observed CODAR currents off of southern Long Island show along-shore westward flow toward New York Harbor, likely setting up the along-shelf pressure gradient for the NJ coast (Fig 10).

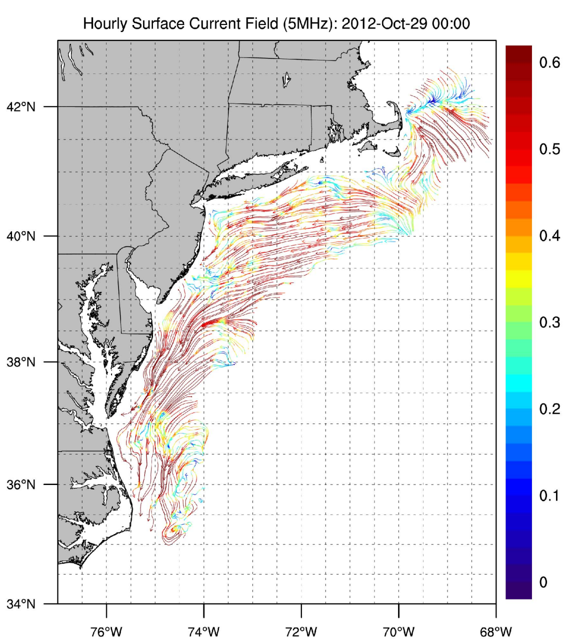

Fig 10. CODAR surface currents on the MAB on October 29th at 00:00 GMT from the 5 MHz network. Colors represent speed and arrows directions.

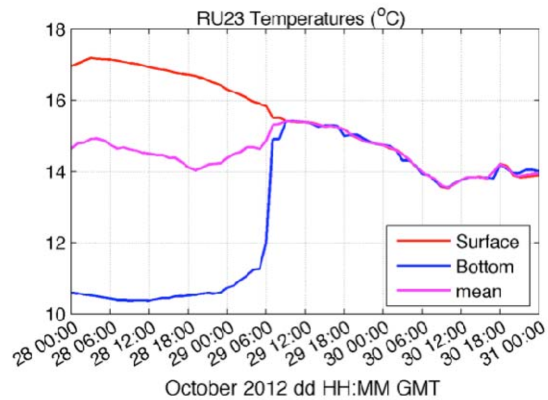

Fig 11. Glider RU23 along-track surface temperature (red), bottom temperature (blue) and mean temperature (magenta) in degrees Celsius.

C. Temperature response

Surface and bottom glider temperatures (Fig 11) show that while bottom temperatures warm drastically, there is a weak surface temperature response at the mid-shelf, with only 2-3C surface cooling despite an almost 8C warming of bottom water. Again this result is consistent with the advection of a downwelling front offshore. Studies by [25] and [29] indicate that the surface temperature sets the water-column temperature as the downwelling front passes. The continued full water-column cooling after it became well-mixed may be a product of atmospheric cooling as air temperatures were generally cooler than water temperatures. [11] indicated that for data assimilation into hurricane forecast models, ocean mean temperature may be more appropriate than simply prescribing a satellite derived SST. While it has yet to be determined whether this method will provide more accurate intensity forecasts when storms cross continental shelves, we treat the mean temperature as proxy for ocean heat-content at the glider location. Mean temperatures at the glider location (Fig 11) actually increased as the thermocline deepened, again consistent with offshore advection of downwelling front and surface water sourced from warmer offshore slope sea waters.

V. Summary and Conclusions

Observations of the coastal ocean response to a large Tropical Cyclone have been severely limited, as extreme weather conditions make sampling difficult. In this paper we detailed the coastal ocean response beneath Hurricane Sandy using a combination of ocean observing assets, most notably a Teledyne-Webb Slocum glider equipped with an upward looking Nortek Aquadopp Current Profiler.

Observations showed that Hurricane Sandy drove a downwelling circulation on the NJ shelf that initiated nearly a full day before the storm made landfall. This downwelling circulation advected cold bottom water offshore and left the inner-shelf well-mixed ahead of the storm, which reduced the ability of coastal sea-surface temperatures to cool significantly ahead of the storm. The cross-shelf force balance was geostrophic, which lead to strong along-shore flow toward the southwest. The along-shelf force balance showed wind stress balanced initially by a combination of forces. As the water-column became well-mixed and sea-levels were elevated in New York Harbor, wind stress and pressure gradient forces were balanced by bottom stress and Coriolis force until the storm passed.

The dynamic ocean response ahead of Hurricane Sandy indicates that fully coupled ocean and atmosphere models may be necessary to accurately forecast hurricane intensity on the MAB, where summer stratification is important. Further observational assets such as gliders and moorings should be included in data assimilation for these models to improve the accuracy the modeled ocean ahead of and during storm events. Future observational work will include downward looking current profilers to more accurately measure bottom stress, and accelerometers to resolve wave motions at glider locations. Continued use of optical sensors is not only critical to resolving environmental properties such as chlorophyll and sediment concentrations, but are also critical for using optical properties as water-mass tracers during extreme events.

Acknowledgements – This work was supported by a Teledyne-Webb Graduate Research Fellowship, a Nortek USA Student Equipment Grant as.

REFERENCES

[1] Glenn, S., Clayton, J., Twardowski, M., Bowers, L., Kerfoot, J., Kohut, J., Webb, D., Schofield, O., 2008. Glider observations of sediment resuspension in a Middle Atlantic Bight Fall transition storm. Limnology and Oceanography 53, 2180–2196.

[2] Travis Miles, Scott M. Glenn, Oscar Schofield, 2012, Temporal and spatial variability in fall storm induced sediment resuspension on the Mid-Atlantic Bight, Continental Shelf Research, Volume 63, Supplement, 15, Pages S36-S49, ISSN 0278-4343,

[3] Styles, R., Glenn, S.M., 2000. Modeling stratified wave-current bottom boundary layers for the continental shelf. Journal of Geophysical Research 105, 24119–24139.

[4] Traykovski, P., Hay, A.E., Irish, J.D., Lynch, J.F., 1999. Geometry, migration, and evolution of wave orbital ripples at LEO-15. Journal of Geophysical Research 104, 1505–1524.

[5] Traykovski, P., 2007. Observations of wave orbital scale ripples and a nonequilibrium time-dependent model. Journal of Geophysical Research 112, C06026.

[6] Babin, S. M., J. A. Carton, T. D. Dickey, and J. D. Wiggert (2004), Satellite evidence of hurricane-induced phytoplankton blooms in an oceanic desert, J. Geophys. Res., 109, C03043, doi:10.1029/2003JC001938.

[7] Xu, Y., Chant, R., Gong, D., Castelao, R., Glenn, S., Schofield, O., 2011. Seasonal variability of chlorophyll a in the Mid-Atlantic Bight. Continental Shelf Research 31, 1640–1650.

[8] Emanuel, Kerry, Christopher DesAutels, Christopher Holloway, Robert Korty, 2004: Environmental Control of Tropical Cyclone Intensity. *J. Atmos. Sci.*, **61**, 843–858.

[9] Bender, M. A., and I. Ginis, 2000: Real-case simulations of hurricane–ocean interaction using a high-resolution coupled model: Effects on hurricane intensity. *Mon. Wea. Rev.,* **128,** 917–946.

[10] Yablonsky, Richard M., Isaac Ginis, 2008: Improving the Ocean Initialization of Coupled Hurricane–Ocean Models Using Feature-Based Data Assimilation. *Mon. Wea. Rev.*, **136**, 2592–2607.

[11] Ali M., Kashyap, T., and P.V. Nagamani, 2013 Use of Sea Surface Temperature for Cyclone Intensity Prediction Needs a Relook, Eos, Vol. 94, No. 19.

[12] Cione, J. J., and E. W. Uhlhorn, 2003: Sea surface temperature variability in hurricanes: Implications with respect to intensity change. *Mon. Wea. Rev.,***131,** 1783–1796.

[13] Jarosz, E., Mitchell, D. A., Wang, D. W., & Teague, W. J. (2007). Bottom-up determination of air-sea momentum exchange under a major tropical cyclone.*Science*, *315*(5819), 1707-1709.

[14] Kohut, J. T., S. M. Glenn, and J. D. Paduan (2006), Inner shelf response to Tropical Storm Floyd, J. Geophys. Res., 111, C09S91.

[15] Ruiz, S., L. Renault, B. Garau, and J. Tintoré (2012), Underwater glider observations and modeling of an abrupt mixing event in the upper ocean, Geophys. Res. Lett., 39, L01603, doi:10.1029/2011GL050078.

[16] Schofield, O., Kohut, J., Aragon, D., Creed, L., Graver, J., Haldeman, C., Kerfoot, J., Roarty, H., Jones, C., Webb, D., Glenn, S., 2007. Slocum gliders: robust and ready. Journal of Field Robotics 24, 473–485.

[17] Visbeck, M. (2002), Deep velocity profiling using lowered acoustic Doppler current profilers: Bottom track and inverse solutions, J. Atmos. Ocean.Technol., 19, 794–807.

[18] Todd, R. E., D. L. Rudnick, M. R. Mazloff, R. E. Davis, and B. D. Cornuelle (2011), Poleward flows in the southern California Current System: Glider observations and numerical simulation, J. Geophys. Res., 116, C02026, doi:10.1029/2010JC006536.

[19] Davis, R.E., Eriksen, C.E., Jones, C.P., 2003. Autonomous buoyancy driven underwater gliders. In: Griffiths, G. (Ed.), Technology and applications of autonomous underwater vehicles. Taylor & Francis, New York, pp. 37–58.

[20] Fairall, C. W., E. F. Bradley, D. P. Rogers, J. B. Edson, and G. S. Young (1996), Bulk parameterization of air-sea fluxes for TOGA COARE, J. Geophys. Res., 101, 3747–3764.

[21] Dzwonkowski, B., Kohut, J.T., Yan, X.-H., 2009b. Sub-inertial characteristics of the surface flow field over the shelf of the central Mid-Atlantic Bight. Continental Shelf Research 29, 1873–1886.

[22] Gong, D., Kohut, J.T., Glenn, S.M., 2010. Seasonal climatology of wind-driven circulation on the New Jersey shelf. Journal of Geophysical Research 115,C04006.

[23] Stewart, R.H., Joy, J.W., 1974. HF radio measurements of surface currents. Deep Sea Research and Oceanographic Abstracts 21, 1039–1049.

[24] Fandry, C. B., and R. K. Steedman (1994), Modelling the dynamics of the transient, barotropic response of continental shelf waters to tropical cyclones, Cont. Shelf Res., 14, 1723–1750.

[25] Lentz, S. J., 2001, The influence of stratification on the wind-driven cross-shelf circulation over the North Carolina Shelf. *J. Phys. Oceanogr.,* **31,** 2749–2760.

[26] Lentz, S., Guza, R.T., Elgar, S., Feddersen, F., Herbers, T.H.C., 1999. Momentumbalances on the North Carolina inner shelf. Journal of Geophysical Research104, 18205–18226.

[27] Kim, S. C., Wright, L. D., & Kim, B. O. (1997). The combined effects of synoptic-scale and local-scale meteorological events on bed stress and sediment transport on the inner shelf of the Middle Atlantic Bight. *Continental Shelf Research*, *17*(4), 407-433.

[28] Grant, W.D., Madsen, O.S., 1979. Combined wave and current interaction with a rough bottom. Journal of Geophysical Research 84, 1797–1808.

[29] Austin JA, Lentz SJ. 2002. The inner shelf response to wind-driven upwelling and downwelling. *J. Phys. Oceanogr.* 32:2171–93.